Applied Surface Science 346 (2015) 574–579

Contents lists available at ScienceDirect

Applied Surface Science

journal homepage: www.elsevier.com/locate/apsusc

Antireflection silicon structures with hydrophobic property fabricated by three-beam laser interference

L. Zhao[a,b], Z. Wang[a,b,*], J. Zhang[a], L. Cao[a], L. Li[a], Y. Yue[a,b,c], D. Li[a,b]

[a] CNM and JR3CN (Changchun University of Science and Technology), Changchun 130022, China
[b] JR3CN (University of Bedfordshire), Luton LU1 3JU, UK
[c] Xi'an Jiaotong-Liverpool University, Suzhou 215000, China

ARTICLE INFO

Article history:
Received 14 February 2015
Received in revised form 1 April 2015
Accepted 7 April 2015
Available online 16 April 2015

Keywords:
Three-beam laser interference
Hexagonal structures
Antireflection
Self-cleaning
Solar cell

ABSTRACT

This paper demonstrates antireflective structures on silicon wafer surfaces with hydrophobic property fabricated by three-beam laser interference. In this work, a three-beam laser interference system was set up to generate periodic micro–nano hole structures with hexagonal distributions. Compared with the existing technologies, the array of hexagonally-distributed hole structures fabricated by three-beam laser interference reveals a design guideline to achieve considerably low solar-weighted reflectance (SWR) in the wavelength range of 300–780 nm. The resulting periodic hexagonally-distributed hole structures have shown extremely low SWR (1.86%) and relatively large contact angle (140°) providing with a self-cleaning capability on the solar cell surface.

1. Introduction

To fabricate solar cells with high conversion efficiency, reduction of the surface reflection is very important. Antireflection coating (ARC) technology is one of the effective methods to achieve high conversion efficiency for crystalline silicon (c-Si) solar cells [1–3]. There are currently various chemical and physical technologies used to modify or pattern silicon wafers for the fabrication of antireflection (AR) surfaces. Alkaline solutions were used to produce a random pyramid texture on crystalline silicon, and silicon nitride (SiNx) thin films were fabricated by plasma enhanced chemical vapor deposition (PECVD) [4,5]. However, these methods have the disadvantages of complexity, high cost and more pollution. Recently, periodic subwavelength scale structures have attracted considerable attention, due to their promising antireflection properties to minimize reflection losses [6–8]. However, they are expensive, only suitable for small area or flat surface applications. Laser interference lithography (LIL) is a potential technology that can produce regular micro–nano structured patterns on silicon wafers for solar cells. This is a simple maskless low-cost and high throughput technology for producing periodic and quasi-periodic silicon structures. Up to now, many efforts have been devoted to study or fabricate micro–nano structures for different applications using LIL. Senthuran et al. [9] reported a maskless and scalable technique for fabricating nano-scale inverted pyramid structures suitable for light management in crystalline silicon solar cells. Zhang et al. [10] fabricated periodic antireflection structures with the average reflectance of 3.5% on silicon using four-beam laser interference lithography. Wang et al. [11] proposed both antireflection and superhydrophobicity structures fabricated by direct laser interference nanomanufacturing and the contact angle and reflectance were 156.3° and 5.9–15.4%. Li et al. [12] presented a method for the fabrication of highly-ordered superhydrophobic micro–nano dual structures on silicon by direct laser interference lithography. The antireflection and self-cleaning functions were due to the formation of an array of micro cone and hole structures on silicon wafer surfaces. Theoretically, using four-beam laser interference method could evenly generate squarely-distributed periodic structure patterns with the antireflection and self-cleaning functions on silicon wafer surfaces, but in practice, noticeable modulations were almost unavoidably introduced in interference patterns due to the misalignment of incident angles or unequal incident angles [13], which is not desired. In contrast to four-beam laser interference, the modulation phenomenon of three-beam laser interference method is not evident, which can avoid the generation of uneven interference patterns and produce the accurate regular interference patterns to ensure the pattern consistency. In addition, the antireflection characteristics of silicon micro–nano structures, fabricated by three-beam laser interference with a

---

[*] Corresponding author at: CNM and JR3CN (Changchun University of Science and Technology), Changchun 130022, China. Tel.: +86 043185582926.
E-mail address: wangz@cust.edu.cn (Z. Wang).

http://dx.doi.org/10.1016/j.apsusc.2015.04.058
0169-4332/© 2015 Elsevier B.V. All rights reserved.

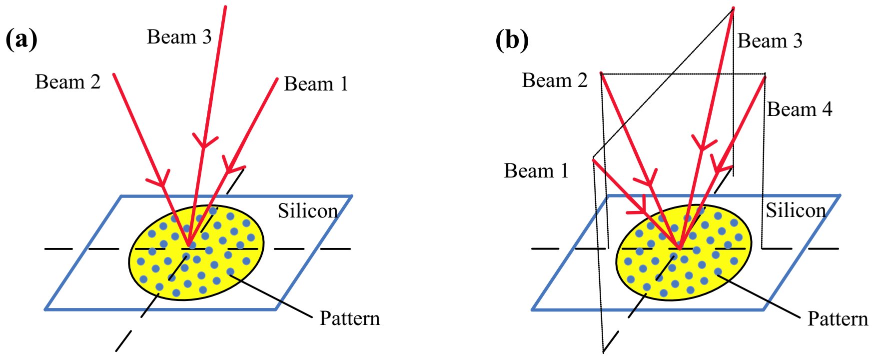

Fig. 1. Schematic diagram of multi-beam laser interference; (a) is the three-beam laser interference and (b) is the four-beam laser interference.

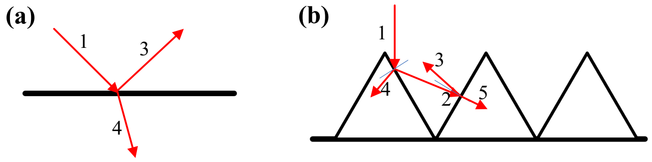

Fig. 2. The principles of the antireflection structures absorbing the sunlight. (a) Is the planar surface and (b) textured surface [15].

hexagonally-distributed array of structures, have not been investigated. Thus, it is worthwhile to study the silicon micro–nano structures to achieve the desirable antireflection silicon structures with hydrophobic property for solar cell applications.

In this work, a three-beam laser interference system was set up to generate periodic micro–nano hole structures with hexagonal distributions. The resulting periodic hexagonally-distributed hole structures have shown extremely low SWR (1.86%) in the wavelength range from 300 nm to 780 nm and relatively large contact angle (140°) providing with a self-cleaning capability on the solar cell surface.

2. Principle

Interference patterns can be arrays or matrices of laser beam lines or dots with different periods, feature sizes and pattern shapes [14]. Fig. 1 shows the configurations of three-beam (a) and four-beam (b) laser interference, and laser beam dots are formed.

The multi-beam interference can be described as the superposition of electric field vectors of three or more laser beams, and it can be written as

$$\vec{E} = \sum_{i=1}^{m} \vec{E}_i = \sum_{i=1}^{m} A_i \vec{P}_i \cos(k\vec{n}_i \cdot \vec{r}_i \pm 2\pi\omega t + \phi_i) \tag{1}$$

where A_i is the amplitude, $\vec{p}_i$ is the unit polarization vector, $k = 2\pi/\lambda$ is the wave number, λ is the wavelength, $\vec{n}_i$ is the unit propagation vector, $\vec{r}_i$ is the position vector, ϕ_i is the phase constant, and ω is the frequency.

The intensity distribution of the interference pattern I can be expressed as

$$I = \sum_{i=1}^{m} |\vec{E}_i|^2 = \sum_{i=1}^{m}\sum_{t=1}^{m} |\vec{E}_i||\vec{E}_t| \cos\langle \vec{E}_i \cdot \vec{E}_t \rangle \tag{2}$$

Fig. 2 shows the principles of the antireflection surface absorbing the sunlight [15].

The period of antireflection structures is defined by [16–18].

$$p < \frac{\lambda_0}{n_{\text{air}} \sin\theta_i \cos\phi + (n^2 - n_{\text{air}}^2 \sin^2\phi)^{1/2}} \tag{3}$$

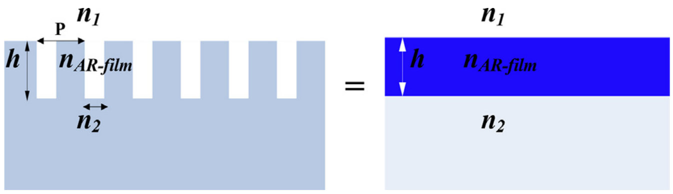

Fig. 3. Sketch of an antireflection film.

where, p is the grating period, λ_0 is the vacuum wavelength, n_{air} is the air refractive index, n is the substrate material refractive index, θ_i is the polar angle of incidence light and ϕ is the azimuthal angle of incidence light.

The maximum period $P_{\max}$, when the incident light is perpendicular to the grating surface, which allows only the propagation of the zero diffraction order, is given by

$$p_{\max} = \frac{\lambda_0}{n} \tag{4}$$

It assumes that the light is incident normally on the top surface. According to the thin-film optics, as shown in Fig. 3, the condition to achieve zero reflection is

$$n_{\text{AR-film}} = (n_1 n_2)^{1/2} \tag{5}$$

$$h = \frac{\lambda}{4n_{\text{AR-film}}} \tag{6}$$

There are three theoretical models for the wetting behavior of a water droplet on the solid surface as shown in Fig. 4. The Young model is valid in the case of a flat solid surface. The Wenzel model is used in the case of a rough surface and the liquid is in the intimate contact with the solid. The Cassie–Baxter model works in the case of the liquid rests on the tops of the asperities [19]. In this paper, the Cassie–Baxter model is used for periodic hexagonally-distributed hole structures.

The Cassie–Baxter model can be written as [19]

$$\cos\ \theta = \psi_L \cos\theta_1 + \psi_A \cos\theta_2 \tag{7}$$

θ_1 and θ_2 are the contact angles of the flat solid and air surfaces, and Ψ_L and Ψ_A are the solid and air surface area fractions of the solid and air surfaces.

3. Experiment

The laser interference system used a seeded Q-switched Nd:YAG laser source with the wavelength of 1064 nm, pulse duration of 7–9 ns, Gaussian beam of 6 mm in diameter and the laser fluence of 637 mJcm^{-2}. The combination of 1/4 wave plates and polarizers were used to control the pulse energy level of single beams and the polarization direction of each beam. The substrates used in